Hindawi
International Journal of Optics
Volume 2023, Article ID 7184080, 10 pages
https://doi.org/10.1155/2023/7184080

Research Article

Optimization and Numerical Modeling of TCO/SnO_2/CdS/CdTe Solar Cells

Parinaz Khaledi[1], **Mahdi Behboudnia**[1], **and Mohammad Karimi**[2]

[1]*Department of Physics, Urmia University of Technology, Urmia, Iran*
[2]*Department of Physics, Shahid Madani University of Azerbaijan, Tabriz, Iran*

Correspondence should be addressed to Parinaz Khaledi; parinaz.khaledi22@gmail.com

Received 14 July 2022; Revised 16 December 2022; Accepted 30 December 2022; Published 12 January 2023

Academic Editor: Yuan-Fong Chou Chau

Due to the excellent performance of the CdTe solar cells, research is ongoing to increase the efficiency of these cells. The first purpose of this study is to increase the accuracy of the physical parameters of a solar cell in the electron-hole production rate equation. In previous studies, this section was neglected because of using only ready-made software. Simulations were performed using a one-dimensional diffusion model in MATLAB and Maple software. Then, in theory, we simulated cadmium telluride-based layered solar cells for the first time without using ready-made software and with coding in MATLAB and Maple software. We designed and optimized the thickness of the layers in solar cells in detail. Then we studied the effect of layer thickness on the short-circuit current (Jsc), open-circuit voltage (Voc), filling factor (FF), and its efficiency. It is found that the efficiency of solar cells layered with TCO/SnO_2/CdS/CdTe layers is as follows: the thickness of the TCO layer is 0.1 μm, that of the SnO_2 layer is equal to 0.1 μm, that of the CdS layer as the window layer is 0.1 μm and the thickness of the CdTe layer as the absorber layer is 3.9 μm. The efficiency of the solar cell with the TCO/SnO_2/CdS/CdTe structure increases significantly and reaches a maximum value of more than 20%.

1. Introduction

Due to limited fossil energy reserves, increasing energy consumption in the world and increasing environmental pollution, we can no longer rely on existing energy sources. Due to these issues and challenges such as increasing efficiency, reducing prices, sustainability, and storage of energy facing renewable energy sources, so many researches have been done. So far, various layered solar cells based on semiconductors have been studied. Recently, perovskite solar cells have been extensively studied theoretically and experimentally [1–7]. Such as the work of Yoo and his colleagues in 2021, the work of Wu and his colleagues in 2020, and other works mentioned in references 1 to 7. Silicon solar cells have also been considered for their high efficiency and stable and nontoxic materials. However, silicon is a material with an indirect energy gap that has a low light absorption coefficient [8]. In contrast, cadmium telluride solar cells have a direct band gap that corresponds to the spectrum of the sun and has excellent performance and a high absorption coefficient [9]. In addition, these cells can be produced at a lower cost than silicon solar cells [10]. All of these properties have attracted scientists' attention to cadmium telluride-based solar cells. In 1982, these cells were examined by a group of researchers [11], they reported a yield of 10% for these cells, but the results of another group [12] showed a yield of 15.8%, and another American laboratory [13] reported the yield to be 16.5%. Recently, returns of 18% and 22% [12, 14], and even returns of 44% have been reported [15]. In cadmium telluride-based solar cells, this layer is often used as an adsorbent layer. This adsorbent layer needs a window layer. The most suitable layer that is used as a window layer next to the cadmium telluride adsorbent layer is cadmium sulfide [16], which forms a PN bond next to cadmium telluride. Cadmium sulfide has a suitable energy gap in the range of 2.42 electron volts. Because cadmium sulfide is a transparent substance, light can penetrate through the cadmium telluride layer, resulting in a photovoltaic effect. Recently, scientists have shown that in addition to experimental approaches, in which optimization is sometimes done experimentally and fails, attempts to analyze device performance through simulation models have shown particular success [17]. The study of solar cell simulations will be very useful for predicting the output performance of solar cells before the actual construction of the cell, and will significantly reduce production costs and avoid excessive costs. Various tools are readily available for simulating solar cells, including wxAMPS, Silvaco ATLAS software, SCAPS-1D software, GPVDM software, and so on. So far, a lot of research has been done and published using these simulation tools [18–25]. But the remarkable point in this field is that with the use of this ready-made software, it is not possible to study the physical equations governing the problem accurately and tangibly. Also, the errors that occur in numerical calculations are not visible. Results are presented only by giving values and constants to the software, which include the absorption coefficient, energy gap and etc., and the software automatically solves equations and does simulation. So far, no study has been done on the simulation of solar cells without the use of ready-made simulation software. In fact, an important feature that distinguishes our work from other studies that have been done so far is avoiding the use of ready-made simulation software. Because optimization requires a proper understanding of physical processes, we first coded in MATLAB and Maple software. Our main goal in this research is to simulate and optimize the different layers used in solar cells. Therefore, in terms of all mathematical and physical parameters, and by simultaneously numerically solving the transport equations, continuity equations, and Poisson equations, we optimized the performance of a multilayer solar cell by calculating unrestricted parameters in terms of independent and limited variables. Layers and their impact on open-circuit voltage, short-circuit current, filling factor, and efficiency have been carefully studied [26].

2. The Governing Physical Equations of the Problem

First, the transport equations, the electron–hole equation, and the Poisson equation must be solved simultaneously. In some previous studies, a quasi-drift diffusion model has been proposed in which only the electron and hole continuity equations were solved, without considering the Poisson equation. The cavity and Poisson equation was, the extended one-dimensionaldrift-diffusion model which can design, optimize, and describe the performance of various cell parameters [27]. The purpose of this paper is to increase the accuracy of a solar cell using the extended drift-diffusion model, adding a layer for optical trapping and thus compensating for the reduction of current, and finally engineering and optimizing the layers to achieve maximum physical accuracy in the parameters of the solar cell [26].

The changes in the electric potential of a semiconductor can be determined from the answer to the Poisson equation.

$$\nabla(\varepsilon\cdot\nabla\Psi)=\rho=q\left(n-p+N_A^{-}-N_D^{+}\right), \tag{1}$$

where Ψ is the electrostatic potential, n, p are the densities of the electron and the hole, N_A^- is the acceptor impurity, and N_D^+ is the impurity.

The densities of electrons and holes in heat balance obey these relations.

$$\begin{aligned} n &= N_C F_{1/2}\left[\frac{\mathbf{E}_{\mathbf{F_n}}-E_C}{KT}\right], \\ p &= N_V F_{1/2}\left[\frac{E_V-\mathbf{E}_{\mathbf{F_p}}}{KT}\right], \\ J_P &= p\mu_p\frac{\mathrm{d}F_p}{\mathrm{d}x}, \\ J_n &= n\mu_n\frac{\mathrm{d}F_n}{\mathrm{d}x}, \end{aligned} \tag{2}$$

where J_n and J_p are the current density of electrons and holes.

$$\begin{aligned} \frac{\partial n}{\partial t} &= \frac{1}{q}\nabla\cdot J_n-U, \\ \frac{\partial p}{\partial t} &= \frac{-1}{q}\nabla\cdot J_p-U. \end{aligned} \tag{3}$$

3. Engineering and Simulated Structure

We first solved the physical equations governing the problem simultaneously, then discretized the equations for coding in MATLAB and Maple software. We simulated important conditions and variables reported in other work [28, 29] for solar cells. We performed the simulation in the conditions of sunlight ($100\,\mathrm{mW\cdot cm^{-2}}$) and mass of world air (AM) 1.5 at a temperature of 300 K.

Figure 1 shows the structure of a simulated CdTe-based solar cell. The structure consists of a transparent TCO conductive oxide layer, a SnO_2 buffer layer, and a CdS and CdTe layer. The n-type CdS layer is used as the window layer, and a p-type CdTe layer is used as the absorbent layer.

The optical band gap, carrier concentration, and other parameters used in simulating the structure of the solar cells were collected from experimental data and other research [9]. The parameters used in this simulation to describe the structure of the simulated CdTe-based solar cells are listed in Table 1.

4. Results and Discussion

4.1. Layer Thickness Engineering. In order to engineer the layer thickness in 4-layer solar cells, including TCO/SnO_2/CdS/CdTe layers, first the mathematical and physical equations governing the problem were solved accurately, then discretizing the equations, in MATLAB and Maple software were done to be performed for programming equations. To ensure the accuracy of the results, equations were solved in both MATLAB and Maple software separately

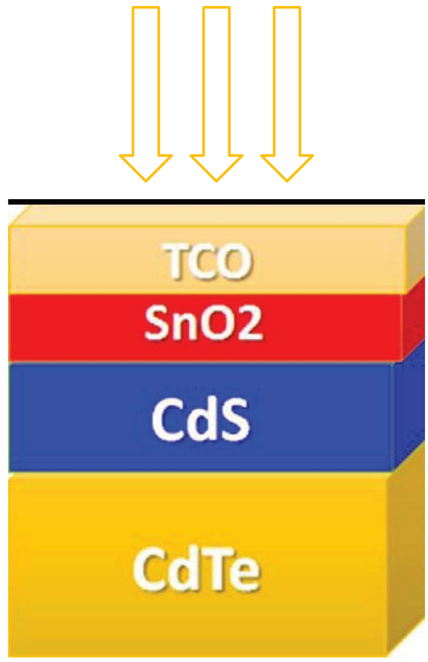

Figure 1: Engineered and simulated solar cell structure.

Table 1: Parameters used in solar cell simulation [9].

Parameter	TCO	SnO_2	CdS	CdTe
Thickness (μm)	0 – 0.5	0.06 – 1	0.1 – 1	0 – 5
Bandgap (ev)	3.6	3.6	2.4	1.5
Electron affinity (ev)	4.5	4.5	4.3	4.28
Dielectric ratio	9	9	10	9.4
Electron mobility (cm^2/Vs)	100	100	100	320
Hole mobility (cm^2/Vs)	25	25	25	40
Valence band effective density of states (cm^{-3})	1.8×10^{19}	1.8×10^{19}	1.8×10^{19}	1.8×10^{19}
Conduction band effective density of states (cm^{-3})	2.2×10^{18}	2.2×10^{18}	2.2×10^{18}	8×10^{17}
Carrier concentration (cm^{-3})	3×10^{20}	—	1×10^{18}	—
Carrier concentration (cm^{-3})	—	—	—	2×10^{14}
Electron lifetime (ns)	100	100	0.01	1
Hole lifetime (ns)	0.1	0.1	0.01	1

and then the results obtained from each software were compared. Additionally, we compare our results with the work done by other researchers in other similar software. The preparation can also be used to analyze and evaluate the results.

The thickness of the layers is one of the important and influential parameters on the electrical properties of solar cells, so first, by considering the data in Table 1, the thickness of the first layer of TCO has been engineered. In Figure 2, the efficiency results in terms of the thickness of the TCO layer are shown. In the range where the thickness of TCO is less than 0.2 μm, the yield is almost constant and from 0.2 to 0.4 μm the yield starts to increase, and at 0.4 μm it reaches its maximum value. For thicknesses greater than 0.4 μm, the first layer of yield starts to reduce again. Therefore, when the thickness of the first layer is 0.4 micrometers, the efficiency of the solar cell reaches its maximum.

Then, considering the thickness of the TCO layer, which is the most efficient for solar cells, the thickness of the second layer of SnO_2 is engineered in terms of efficiency. The thickness of the second layer in terms of efficiency is shown in Figure 3. As shown in Figure 3, at a thickness of 0.1 of the second layer, the efficiency of the solar cell reaches its maximum value, and for thicknesses greater than 0.1 micrometers, the efficiency begins to decrease.

The third layer that we used in the structure of the solar cell is the CdS layer. This layer has a suitable energy gap in the range (2.42–3.1 ev). Due to its suitable chemical properties, it is often used as a window layer in the structure of solar cells. Figure 4 shows the efficiency of the solar cell in terms of the thickness of the window layer. As shown in this figure, when the window layer thickness is greater than 0.1 micrometers, the efficiency of the solar cell begins to decrease, and at a thickness of 0.1 micrometers for the window layer, the efficiency reaches its maximum value.

Table 2 shows the thickness of layers in Figures 5–7. Other physical parameters used are listed in Table 1.

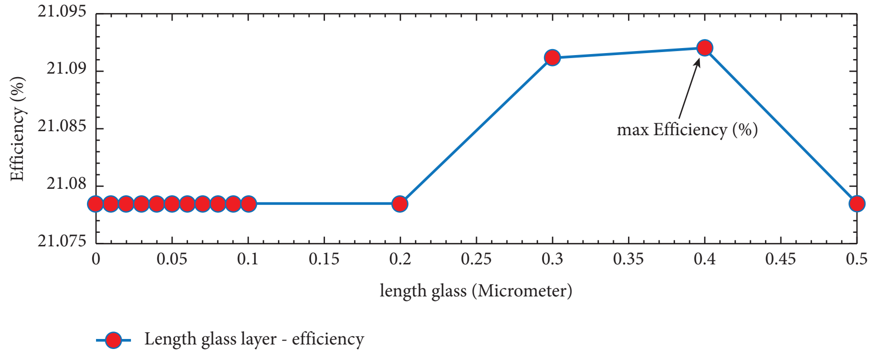

Figure 2: Efficiency diagram in terms of TCO layer thickness.

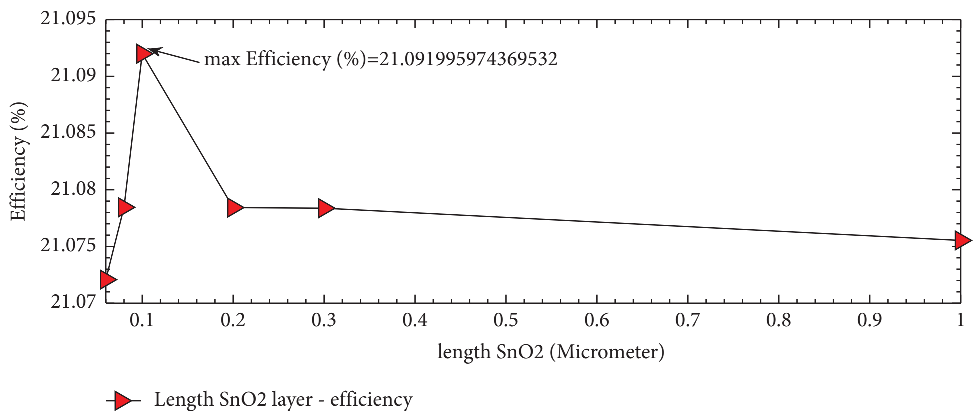

Figure 3: Performance diagram in terms of SnO_2 layer thickness.

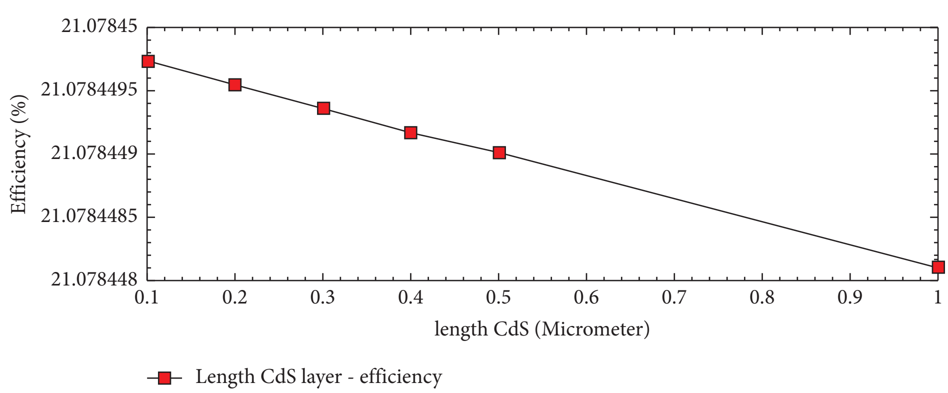

Figure 4: Performance chart in terms of CdS layer thickness.

Table 2: The thickness of the layers in Figures 5–7.

Parameter	TCO	SnO_2	CdS	CdTe
Thickness (μm)	0.4	0.1	0.2 – 0.8	3

We considered the thickness of the first, second, and fourth layers as 0.4 micrometers, 0.1 micrometers, and 3 micrometers, respectively, and we changed the thickness of the third layer from 0.2 micrometers to 0.8 micrometers, and the changes in the filling and flow coefficients We showed the short circuit and open-circuit voltage according to the thickness change of the third layer in Figures 5–7, respectively.

The fourth layer that is engineered in the structure of our solar cells is the CdTe layer. This layer is used as the absorber layer. CdTe plays the role of the adsorbent layer in the structure of solar cells due to its high and suitable absorption coefficient. Figure 8 shows the efficiency diagram in terms of the thickness of the adsorbent layer. The absorbent layer thickness was carefully engineered in

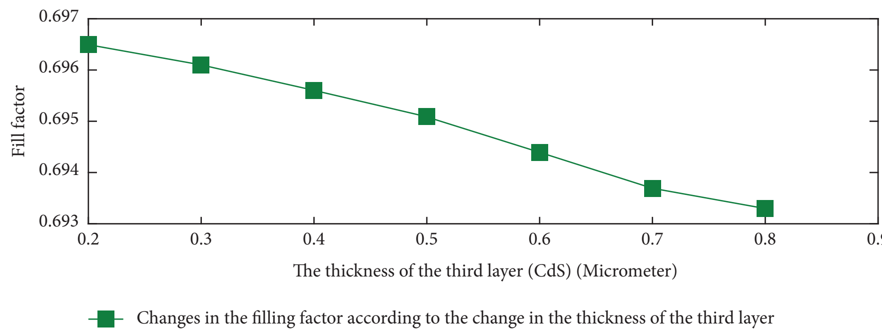

Figure 5: Graph of the filling factor according to the thickness of the CdS layer.

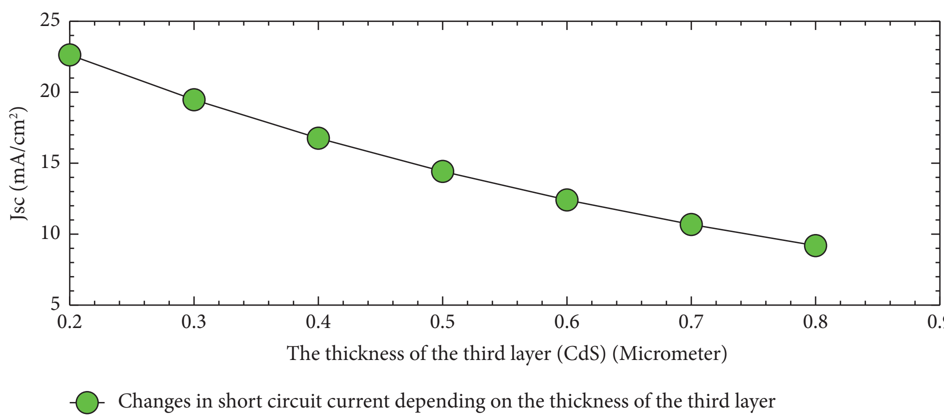

Figure 6: Short-circuit current diagram according to CdS layer thickness.

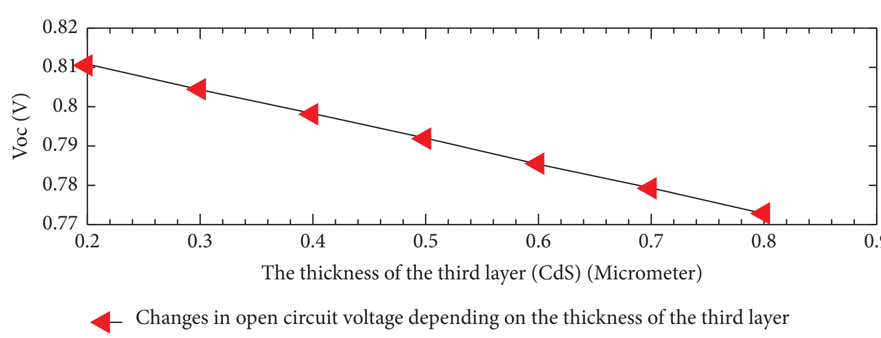

Figure 7: Open-circuit voltage diagram according to the thickness of the CdS layer.

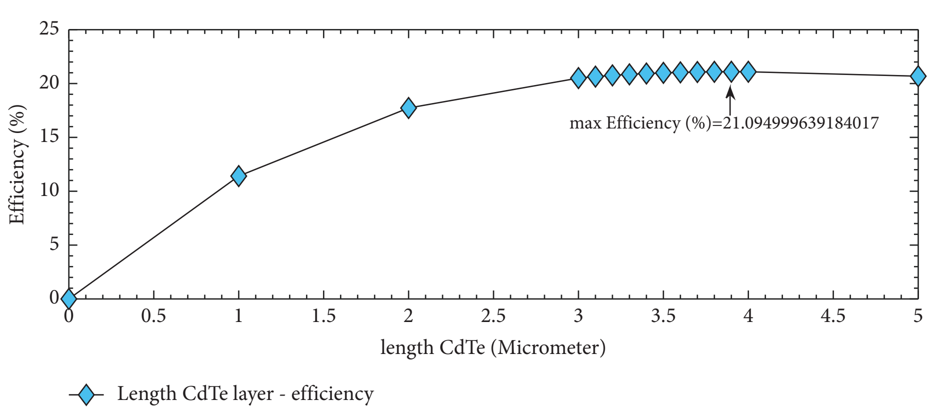

Figure 8: Performance diagram in terms of CdTe layer thickness.

Table 3: The thickness of the layers in Figures 9–11.

Parameter	TCO	SnO_2	CdS	CdTe
Thickness (μm)	0.4	0.1	0.1	0.2 – 4

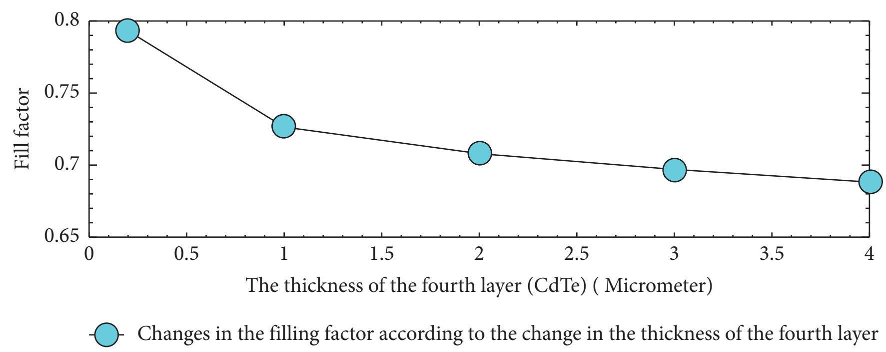

Figure 9: Graph of the filling factor according to the thickness of the CdTe layer.

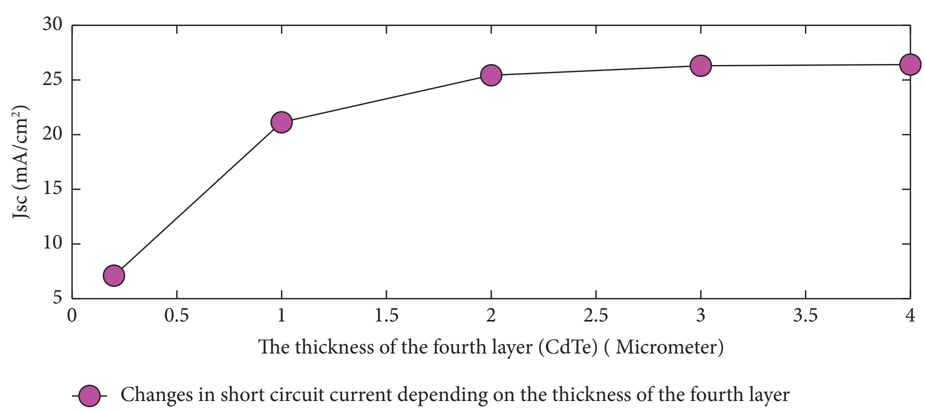

Figure 10: Short-circuit current diagram according to CdTe layer thickness.

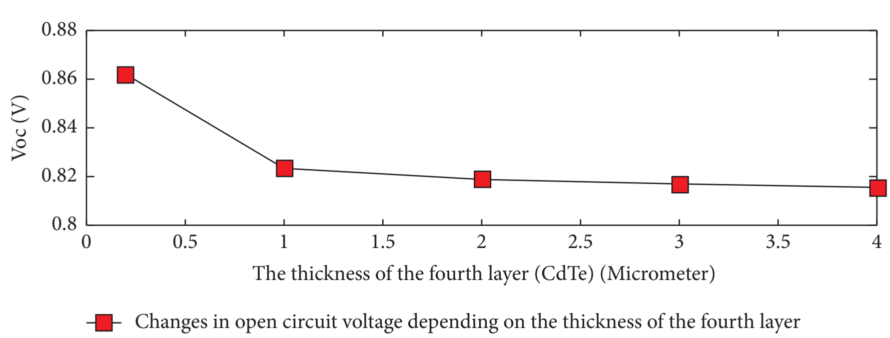

Figure 11: Open-circuit voltage diagram according to the thickness of the CdTe layer.

the range of zero to 5 micrometers. From a thickness of 0 to 3.9 μm for the absorber layer, the efficiency increases, and at a thickness of 3.9 μm CdTe, the efficiency of the solar cell reaches its maximum. The efficiency is then reduced for thicknesses greater than 3.9 μm for the adsorbent layer.

Table 3 shows the thickness of the layers in Figures 9–11. Other physical parameters used are listed in Table 1.

We considered the thickness of the first, second, and third layers as 0.4 micrometers, 0.1 micrometers, and 0.1 micrometers, respectively, and we changed the thickness of the fourth layer from 0.2 micrometers to 4 micrometers, and the changes in the filling and flow coefficients We showed the short circuit and open-circuit voltage according to the thickness change of the fourth layer in Figures 9–11, respectively.

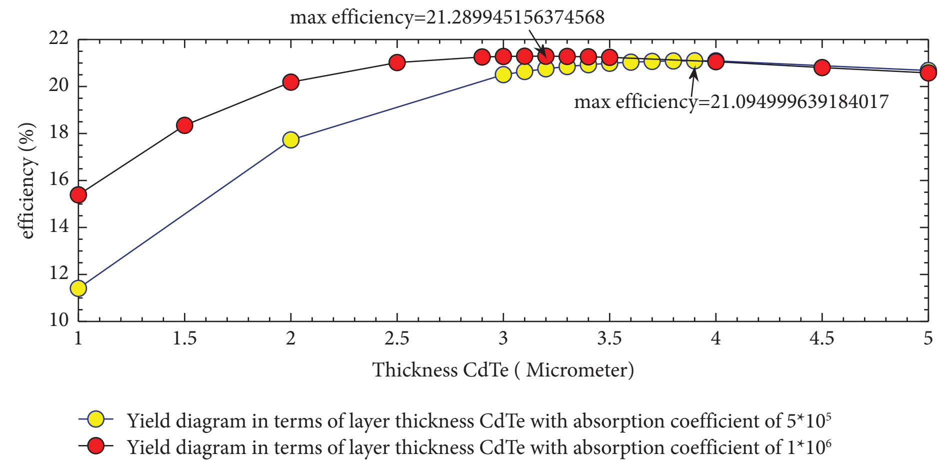

Figure 12: Performance diagram in terms of CdTe layer thickness in two modes with different absorption coefficients.

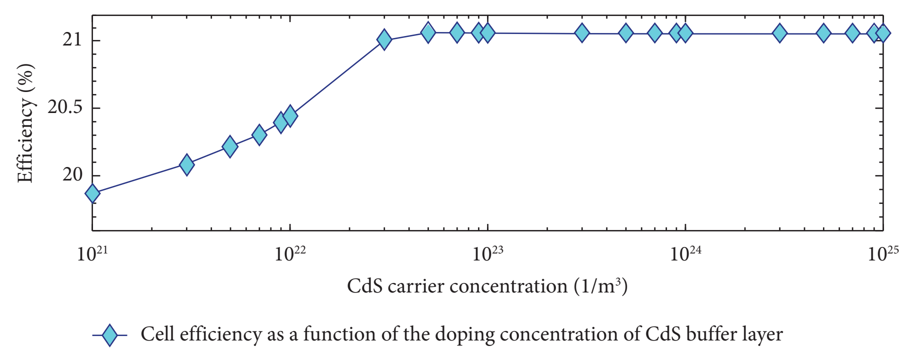

Figure 13: Efficiency in terms of window layer thickness.

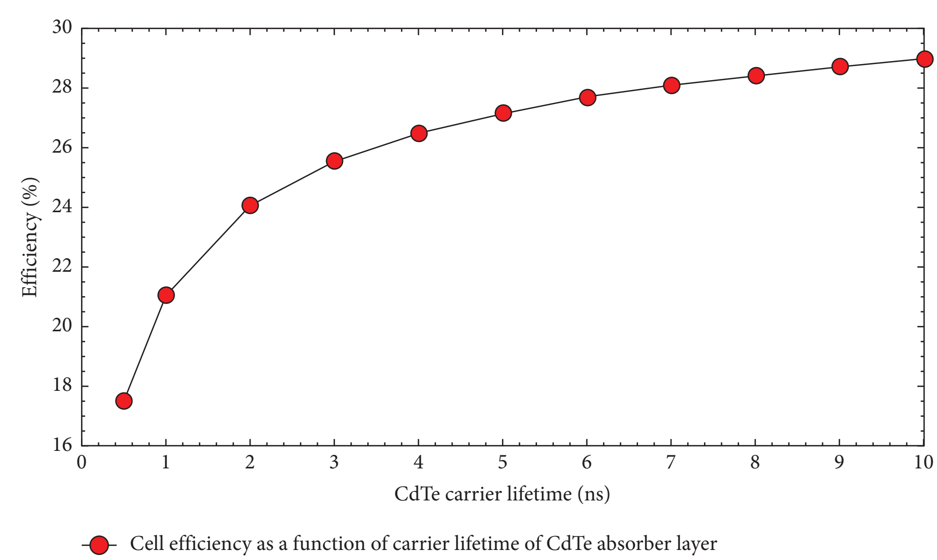

Figure 14: Solar cell efficiency in terms of carrier lifespan in the absorber layer.

Different values were reported [30, 31] for the CdTe adsorption coefficient, in previous studies. Therefore, we examined the reports in the previous works one by one, and after comparing them, we chose the value that would give the maximum return in our work. Figure 12 shows the efficiency diagram in terms of the absorption coefficient of the adsorbent layer.

Figure 13 shows the efficiency of a solar cell in terms of the impurity of the window layer. The impurity of the cadmium sulfide layer is examined as the window layer from

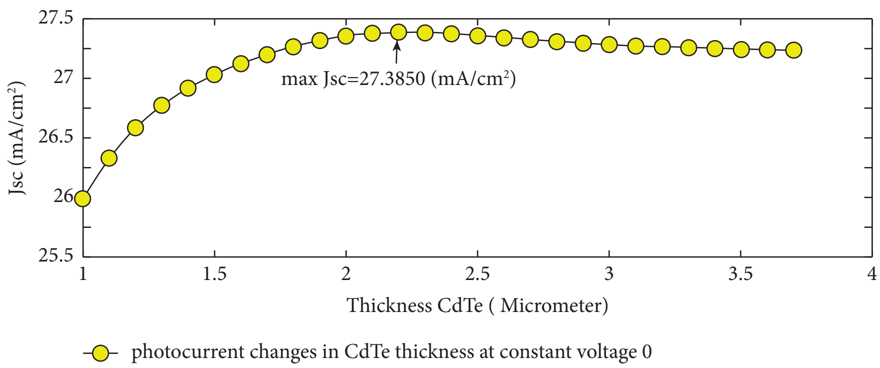

Figure 15: Short-circuit current in terms of the thickness of the absorber layer at a constant voltage of zero v.

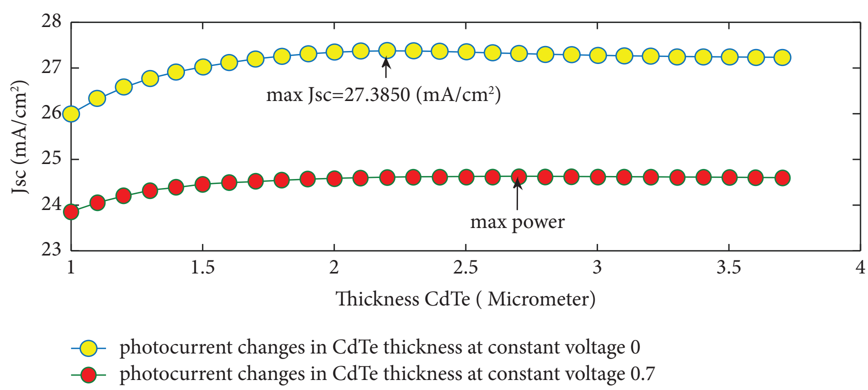

Figure 16: Short-circuit current according to the thickness of the absorber layer at two constant voltages of 0 and 0.7 V.

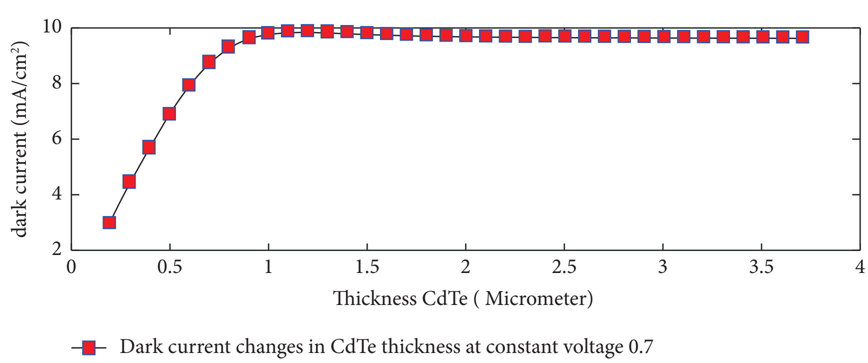

Figure 17: Dark current in terms of the thickness of the absorber layer at a constant voltage of 0.7 volts.

$(10^{21}$ to $10^{25})1/m^3$. As shown in Figure 13, the efficiency is increased from 10^{21} to $10^{23}\,1/m^3$ and from 10^{23} to $10^{25}\,1/m^3$ is almost constant.

Carrier lifespan is another important parameter that has a significant impact on the efficiency of solar cells. In Figure 14, we showed the lifespan of carriers in the absorber layer in terms of solar cell performance.

Another important parameter that affects the efficiency of solar cells is the zero resistance current or in other words the short-circuit current. First, at a zero constant voltage, we examined the short-circuit current in terms of the thickness of the absorber layer, the results of which are shown in Figure 15. Then, we studied the short-circuit current in terms of the thickness of the absorber layer, at a constant voltage of 0.7 volts. We compare the short-circuit current in terms of the thickness of the absorber layer at two constant voltages of 0 and 0.7 volts and combined both results in Figure 16.

Dark current is another important parameter that is usually less considered in articles. In Figure 17, at a constant voltage of 0.7 volts, we studied the dark current in terms of the thickness of the absorber layer.

5. Conclusion

So far, many studies have been done on the numerical simulation and optimization of solar cells, most of which have been prepared using simulation software. For the first time, in a completely different way and with accurate consideration of mathematical and physical equations, we simulate these equations ourselves. Rule without using ready-made software packages for simulation, 4-layer TCO/ SnO_2/CdS/CdTe solar cells were simulated by solving equations and then discretization and programming in MATLAB and Maple software. Then, for optimization, various parameters such as the thickness of each of the four layers were studied carefully. The results showed that a 4-layer solar cell with TCO/SnO_2/CdS/CdTe layers with a total thickness of 4.5 microns can be efficient by more than 20%.

Data Availability

Data are available upon request to the corresponding author.

Conflicts of Interest

The authors declare that they have no conflicts of interest.

Acknowledgments

This work was supported by the Department of Physics, Urmia University of Technology.

References

[1] J. J. Yoo, G. Seo, M. R. Chua et al., "Efficient perovskite solar cells via improved carrier management," *Nature*, vol. 590, no. 7847, pp. 587–593, 2021.

[2] B. B. Yu, Z. Chen, Y. Zhu et al., "Heterogeneous 2D/3D thalides perovskite solar cells with certified conversion efficiency breaking 14%," *Advanced Materials*, vol. 33, no. 36, Article ID 2102055, 2021.

[3] X. Jiang, H. Li, Q. Zhou et al., "One-step synthesis of $SnI_2{\cdot}(DMSO)_x$ adducts for high-performance tin perovskite solar cells," *Journal of the American Chemical Society*, vol. 143, no. 29, pp. 10970–10976, 2021.

[4] T. Wu, Z. Qin, Y. Wang et al., "The main progress of perovskite solar cells in 2020–2021," *Nano-Micro Letters*, vol. 13, no. 1, pp. 152–218, 2021.

[5] Q. Cao, Y. Li, H. Zhang et al., "Efficient and stable inverted perovskite solar cells with very high fill factors via incorporation of star-shaped polymer," *Science Advances*, vol. 7, no. 28, Article ID eabg0633, 2021.

[6] S. Seo, S. Shin, E. Kim, S. Jeong, N. G. Park, and H. Shin, "Amorphous TiO2 coatings stabilize perovskite solar cells," *ACS Energy Letters*, vol. 6, no. 9, pp. 3332–3341, 2021.

[7] J. Jeong, M. Kim, J. Seo et al., "Pseudo-halide anion engineering for α-FAPbI3 perovskite solar cells," *Nature*, vol. 592, no. 7854, pp. 381–385, 2021.

[8] R. Saive, "Light trapping in thin silicon solar cells: a review on fundamentals and technologies," *Progress in Photovoltaics: Research and Applications*, vol. 29, no. 10, pp. 1125–1137, 2021.

[9] I. E. Tinedert, A. Saadoune, I. Bouchama, and M. A. Saeed, "Numerical modelling and optimization of CdS/CdTe solar cell with incorporation of Cu2O HT-EBL layer," *Optical Materials*, vol. 106, Article ID 109970, 2020.

[10] D. K. Shah, D. Kc, M. Muddassir, M. S. Akhtar, C. Y. Kim, and O. B. Yang, "A simulation approach for investigating the performances of cadmium telluride solar cells using doping concentrations, carrier lifetimes, thickness of layers, and band gaps," *Solar Energy*, vol. 216, pp. 259–265, 2021.

[11] Y. S. Tyan and E. A. Perez-Alburne, "Efficient thin-film CdS/ CdTe solar cells," in *Proceedings of the Conf. Rec. IEEE Photovoltaic Spec. Conf.;(United States) (No. CONF-820906-)*, Rochester, NY, September 1982.

[12] C. S. Ferekides, J. Britt, Y. Ma, and L. Killian, "High efficiency CdTe solar cells by close spaced sublimation," in *Proceedings of the Conference Record of the Twenty Third IEEE Photovoltaic Specialists Conference-1993 (Cat. No. 93CH3283-9)*, pp. 389–393, IEEE, Louisville, Kentucky, May 1993.

[13] X. Wu, "High-efficiency polycrystalline CdTe thin-film solar cells," *Solar Energy*, vol. 77, no. 6, pp. 803–814, 2004.

[14] N. Romeo, A. A. Bosio, and A. Romeo, "An innovative process suitable to produce high-efficiency CdTe/CdS thin-film modules," *Solar Energy Materials and Solar Cells*, vol. 94, no. 1, pp. 2–7, 2010.

[15] A. Kuddus, A. B. M. Ismail, and J. Hossain, "Design of a highly efficient CdTe-baseddual-heterojunction solar cell with 44% predicted efficiency," *Solar Energy*, vol. 221, pp. 488–501, 2021.

[16] W. K. Metzger, S. Grover, D. Lu et al., "Exceeding 20% efficiency with in situ group V doping in polycrystalline CdTe solar cells," *Nature Energy*, vol. 4, no. 10, pp. 837–845, 2019.

[17] A. Rohatgi, B. Rounsaville, Y. W. Ok et al., "Fabrication and modeling of high-efficiency front junction n-type silicon solar cells with tunnel oxide passivating back contact," *IEEE Journal of Photovoltaics*, vol. 7, no. 5, pp. 1236–1243, 2017.

[18] Y. Liu, Y. Sun, and A. Rockett, "A new simulation software of solar cells—wxAMPS," *Solar Energy Materials and Solar Cells*, vol. 98, pp. 124–128, 2012.

[19] S. Michael and A. Bates, "The design and optimization of advanced multijunction solar cells using the Silvaco ATLAS software package," *Solar Energy Materials and Solar Cells*, vol. 87, no. 1-4, pp. 785–794, 2005.

[20] S. Michael, A. D. Bates, and M. S. Green, "Silvaco ATLAS as a solar cell modeling tool," in *Proceedings of the Conference Record of the Thirty-first IEEE Photovoltaic Specialists Conference*, pp. 719–721, IEEE, Lake Buena Vista, FL, USA, January 2005.

[21] M. Mostefaoui, H. Mazari, S. Khelifi, A. Bouraiou, and R. Dabou, "Simulation of high efficiency CIGS solar cells with SCAPS-1D software," *Energy Procedia*, vol. 74, pp. 736–744, 2015.

[22] A. Kumar Mishra and R. K. Shukla, "Electrical and optical simulation of typical perovskite solar cell by GPVDM software," *Materials Today Proceedings*, vol. 49, pp. 3181–3186, 2022.

[23] J. Qu, L. Zhang, H. Wang, X. Song, Y. Zhang, and H. Yan, "Simulation of double buffer layer on CIGS solar cell with SCAPS software," *Optical and Quantum Electronics*, vol. 51, no. 12, pp. 383–414, 2019.

[24] A. Fell, J. Schön, M. C. Schubert, and S. W. Glunz, "The concept of skins for silicon solar cell modeling," *Solar Energy Materials and Solar Cells*, vol. 173, pp. 128–133, 2017.

[25] M. Elbar and S. Tobbeche, "Numerical simulation of CGS/ CIGS single and tandem thin-film solar cells using the Silvaco-Atlas software," *Energy Procedia*, vol. 74, pp. 1220–1227, 2015.

[26] P. Khaledi, M. Behboodnia, and M. Karimi, "Simulation and optimization of temperature effect in solar cells CdTe with back connection Cu2O," *International Journal of Optics*, vol. 2022, pp. 1–10, 2022.

[27] P. Khaledi and Y. Abedini, "Simulation and Investigation of the Optical Properties of cds/cdte solar cells," in *Proceedings of the International Conference on Optoelectronic, Applied Optics*

*and Microelectronics (OAM-2019)*þ, Kolkata, India, August 2019.

[28] S. Ahmmed, A. Aktar, J. Hossain, and A. B. M. Ismail, "Enhancing the open circuit voltage of the SnS based heterojunction solar cell using NiO HTL," *Solar Energy*, vol. 207, pp. 693–702, 2020.

[29] S. Ahmmed, A. Aktar, M. F. Rahman, J. Hossain, and A. B. M. Ismail, "A numerical simulation of high efficiency CdS/CdTe based solar cell using NiO HTL and ZnO TCO," *Optik*, vol. 223, Article ID 165625, 2020.

[30] J. Pantoja Enriquez, N. R. Mathews, G. Pérez Hernández, and X. Mathew, "Influence of the film thickness on structural and optical properties of CdTe thin films electrodeposited on stainless steel substrates," *Materials Chemistry and Physics*, vol. 142, no. 1, pp. 432–437, 2013.

[31] M. F. Al-Kuhaili, "Photoelectric properties of highly conductive samarium-doped cadmium telluride thin films for photovoltaic applications," *Solar Energy*, vol. 213, pp. 163–171, 2021.